ChemPubSoc Europe

DOI: 10.1002/chem.201500101

CHEMISTRY
A European Journal
Communication

Self-Assembly

Supramolecular Capsules from Bilayer Membrane Scission Driven by Corannulene

Yongju Kim and Myongsoo Lee*[a]

Abstract: Self-assembly of polyaromatic systems has proved to be a powerful technique to construct nanoscale optoelectronic materials. However, attempts to develop self-assembled nanomaterials guided by pristine polyaromatic molecules have been limited. Here the construction of photoactive nanocapsules through the scission of an aromatic bilayer membrane driven by curved corannulene intercalation is reported. The framework of the capsule consists of the lateral array of corannulene, a buckyball fragment. The supramolecular capsules exhibit photocatalytic activity to degrade encapsulated fluorescein dye molecules under sunlight irradiation.

Supramolecular systems based on noncovalent bonds are adaptive due to the reversible nature of the noncovalent interactions, enabling stimuli responsiveness and self-healing.[1] Our efforts to design supramolecular structures with dynamic characteristics can introduce novel properties in target nanomaterials that are extremely useful in smart materials and living systems.[2] A well-known example of supramolecular assembly in nature is the formation of plasma membranes, in which protein and lipid molecules are held together by cooperative noncovalent interactions.[3] Cell membranes serve many important functions indispensable for life, such as transport, energy storage, and information transduction.[4] For transport of molecules, membranes are able to separate to take up, transport, and release molecules through budding and scission dynamics triggered by clathrin binding.[5] The binding of curved clathrin proteins to large plasma membranes enforces planar membrane structures to be highly curved, eventually to break-up into small vesicular pockets. With such an example from nature as a guide, controlled self-assembly is becoming more and more a laboratory tool for the construction of dynamic nanoscopic structures that mimic biological systems.[6]

Various responsive supramolecular structures are able to be formed by self-assembly of small block molecules based on rigid aromatic segments.[2] In contrast to conventional block copolymers and lipid amphiphiles, additional noncovalent interactions of the aromatic segments endow self-assembled structures with dynamic responsive properties without collapse of their structural integrity. For example, rationally designed supramolecular tubules are able to undergo reversible switching between expanded and contracted states through a molecular sliding motion of the aromatic segments with chirality inversion in response to a thermal trigger.[7] In the case of helically folded nanofibers, environmental changes trigger their folded structures to unfolded states through conformational change of aromatic segments.[8] The porous capsules formed by self-assembly of dumbbell-shaped aromatic amphiphiles undergo open/closed gating motion triggered by external stimuli.[9] Lateral attachment of the dendritic oligo(ethylene oxide) segments into an aromatic rod leads the molecules to self-assemble into foldable sheets that reversibly roll-up into scrolled tubules triggered by temperature.[10] The entropically driven dehydration of the oligoether chains triggers this structural change to reduce dehydrated surface area that is exposed to water environment.

2D self-assembled dynamic structures can be also constructed by self-assembly of face-on-grafted disk-shaped aromatic amphiphiles.[11] The basal-plane chains grafted the aromatic segment enforce the molecules to be faced with each other to form small dimeric micelles with hydrophilic up and down and hydrophobic side faces. The dimeric micelles in turn grow in only *x*–*y* directions through side-to-side hydrophobic interactions to form dynamic porous sheets. The lateral pores undergo an open/closed gating motion in response to flat coronene guest intercalation without compromising the 2D integrity of the supramolecular structure. This observation together with membrane scission driven by curved proteins in nature stimulated us to envision that the curved guests such as corannulene would function as a trigger for the scission of the 2D supramolecular structures through a budding process. Herein we present the scission of a 2D bilayer aromatic membrane into supramolecular capsules through bud formation triggered by corannulene intercalation (Figure 1).

The self-assembling molecule that forms 2D membrane structures consists of a conformationally flexible, macrobicyclic aromatic segment and a hydrophilic oligoether dendron grafted on its basal plane. The synthesis of face-on grafted aromatic amphiphile **1** was performed according to the procedures described previously.[11] In aqueous solution, the molecule self-assembles into porous sheets through the dimeric micelles as an intermediate structure. The dimeric micelles based on faced aromatic pairs are expected to encapsulate curved aromatic guest molecules through conformational change to fit the curvature of the guest. Indeed, the aqueous solution of **1** readily

[a] *Dr. Y. Kim, Prof. Dr. M. Lee*
State Key Laboratory for Supramolecular Structure and Materials
College of Chemistry, Jilin University, Changchun 130012 (China)
E-mail: mslee@jlu.edu.cn

Supporting information for this article is available on the WWW under http://dx.doi.org/10.1002/chem.201500101.

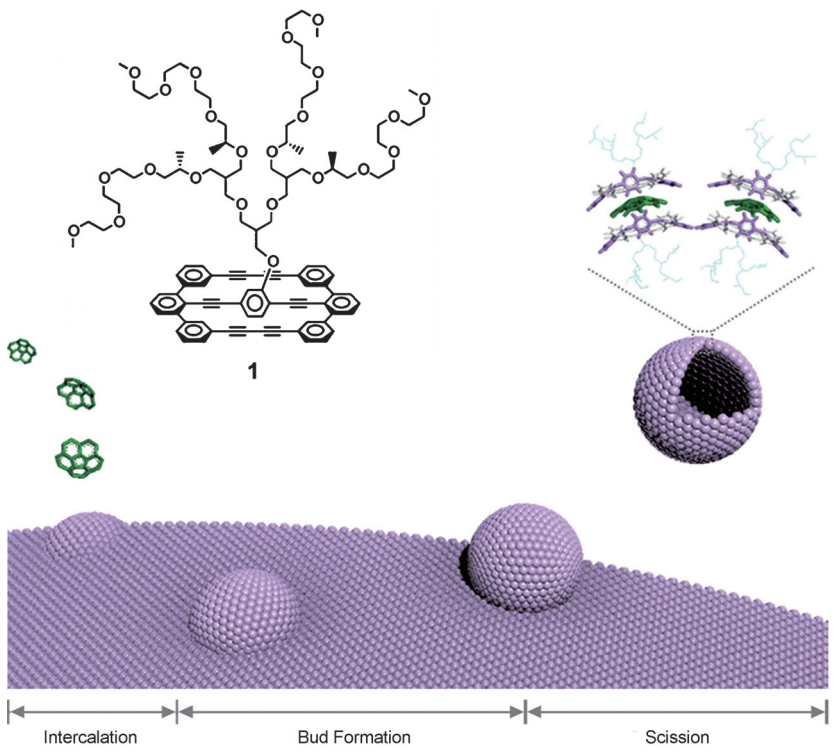

Figure 1. Molecular structure of amphiphile **1** composed of a macrobicyclic aromatic segment with oligoether-basal plane dendron and schematic illustration of the scission of a bilayer membrane through a budding process.

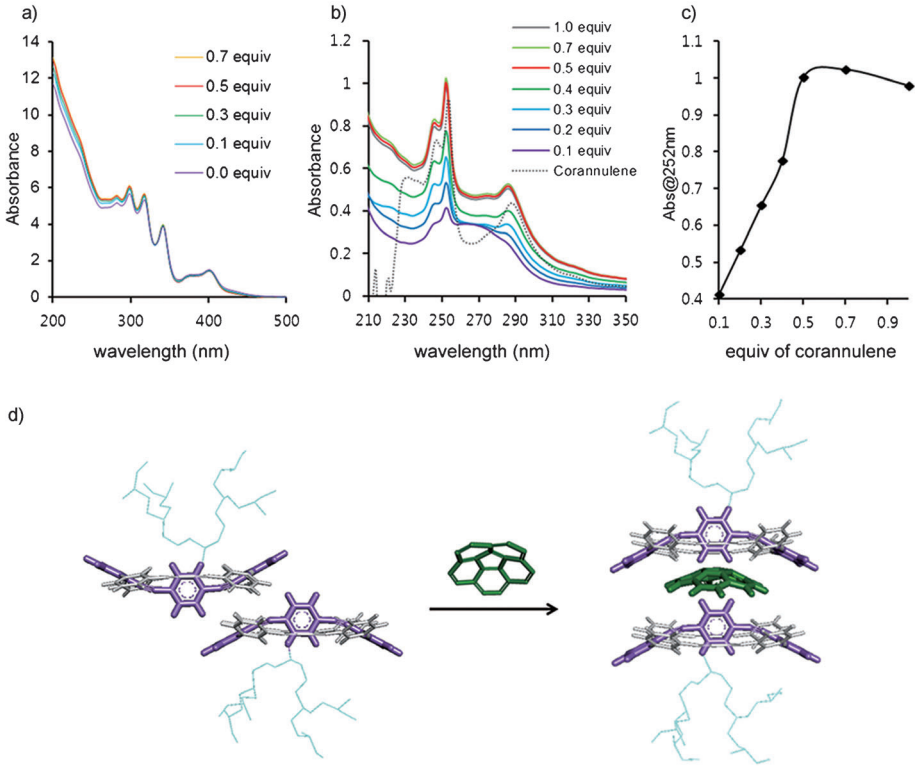

Figure 2. a) Absorption spectra of aqueous solutions **1** (50 μM) in the presence of different equivalents of corannulene. b) Absorption spectra after subtracting 0.0 equivalents of corannulene sample from the samples with different equivalents of corannulene, indicative of the presence of corannulene. The dotted line is the 25 μM corannulene solution in $CHCl_3$. c) The plot of absorption at 252 nm versus the different equivalents of corannulene shows that the maximum amount of corannulene loading is 0.5 equivalents. d) Energy calculation result that shows the conformational inversion of one of the macrobicycles upon corannulene intercalation.

solubilized curved corannulene guest with up to 0.5 equivalents of the guest molecule. Upon addition of corannulene to the aqueous solution of **1**, the absorbance at 252 nm associated with corannulene increases up to 0.5 equivalents, beyond which the absorbance did not change with noticeable precipitation upon further addition of the guest to the solution (Figure 2a–c). This result indicates that the maximum amount of corannulene loading per amphiphilic molecule is 0.5 equivalents, which implies that the curved aromatic guest is sandwiched between the two aromatic basal planes of the dimeric micelle through the conformational change of one of the aromatic macrobicyles.

To corroborate the conformational change of the aromatic basal planes upon intercalation of the corannulene guest, we have performed molecular-modeling experiments. The energy minimization shows that one of the aromatic planes adopts an inverted boat conformation with a protruded central benzene ring toward the dendrimer side when they encapsulate corannulene, different from the dimeric micelle without guest encapsulation (Figure 2d). As a result, this conformational inversion of the boat conformation provides an appropriate internal cavity to intercalate a corannulene molecule efficiently. This curved arrangement of the paired aromatic macrobicycles in a direction perpendicular to the basal plane is reflected in the transformation of highly curved capsules upon the addition of curved corannulene, which will be discussed later.

To investigate the influence of the corannulene intercalation on the 2D membrane structure, we have performed dynamic light scattering (DLS) experiments with the solution of **1** containing

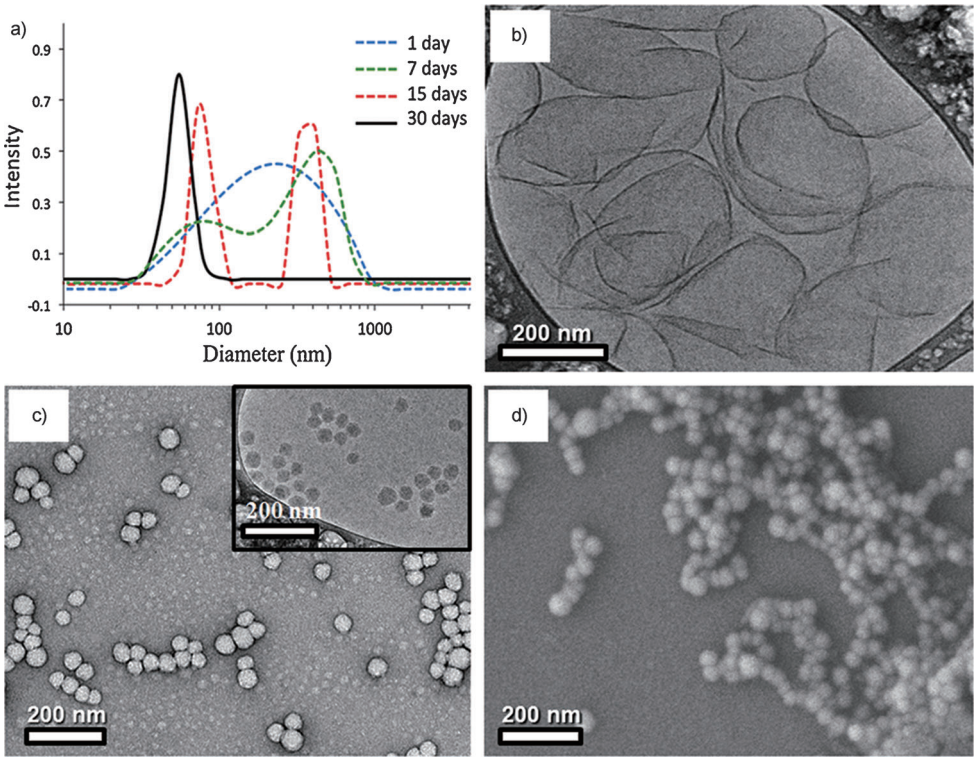

Figure 3. a) Size-distribution graph from DLS measurements of aqueous solutions **1** (50 μM) with 0.5 equivalents of corannulene at different time intervals. b) Cryogenic-TEM (Cryo-TEM) image of 2D membrane from a solution of **1** (50 μM) without corannulene. c) TEM image and d) SEM image of capsules after one month aging time from the aqueous solutions **1** (50 μM) with 0.5 equivalents of corannulene. The inset of (c) is a cryo-TEM image.

0.5 equivalents of corannulene. Remarkably, addition of 0.5 equivalents of the guest with respect to **1** triggers the large aggregates to significantly decrease in hydrodynamic diameter from several hundred nanometers to 59 nm with a uniform size distribution (Figure 3a). The TEM images reveal that, upon intercalation of the curved guest, the membrane structures (Figure 3b) completely transform into uniform vesicular micelles with an average diameter of 57 nm (Figure 3c), which is consistent with the DLS results. SEM experiments further corroborate this result, which shows the formation of small spherical objects with highly uniform diameters of ~60 nm (Figure 3d). These results indicate that the intercalation of curved guest enforces the large membrane to break-up into small capsules, in which the framework consists of a lateral arrangement of corannulene, a buckyball fragment.

To gain insight into the scission mechanism of the 2D aromatic membranes, we have performed TEM investigations of the sample containing 0.5 equivalents of the corranulene guest over one month (Figure 4). Until two day aging after the addition of the guest, the flat membrane structures remain unchanged. After three days, the membranes begin to deform into buds, in which the curvature steadily increases. After one month aging, the buds brake up into isolated capsules, which indicates that the flat supramolecular membranes split up into small capsules passing through bud formation at intermediate stages. As described in the earlier part, the conformationally flexible aromatic macrobicycles are loosely faced in the dimeric micelles due to steric interference between the protruded central phenyl groups. To be more closely packed, the dimeric micelles allow corannulene to be intercalated through the conformational change of the macrobicycles to optimize π–π-stacking between the aromatic systems in aqueous solution. Thus, the intercalation of corannulene leads to the preferred curvature of the dimeric micelles with enhanced hydrophobic side faces (Figure 2d). Subsequently, the strengthened side by side hydrophobic interactions between the curved micelles enforces the loosely packed bilayers to be curved to transform capsules. The formation of highly uniform capsules reflects the presence of the preferred curvature of the primary micelles driven by curved corannulene. This scission mechanism driven by curved guest is similar to that of plasma membrane scission driven by clathrin proteins in nature.[12]

To substantiate encapsulation capability of the capsules into their hollow cavities, we have performed encapsulation experiments with fluorescein. Fluorescein was added to the aqueous solution of **1** containing 0.5 equivalents of corannulene in which the self-assembled structures exist as open forms. The resulting solution was aged for one month, in which the open structures are closed to the capsules. After the filtration of free fluorescein by using a Sephadex column, the solution was subjected to UV/Vis measurements. The spectrum showed an additional peak at 490 nm in the visible region (Figure 5a, 0 h), which indicates that the fluorescein molecules are encapsulated within the internal cavity of the capsule.

The supramolecular capsules could function as a photocatalyst for degradation of organic dye molecules because the intercalated corannulene guest serves as an acceptor of the electrons generated in conjugated molecules **1**.[13] The photocatalytic degradation of fluorescein was subsequently investigated in aqueous solution of the capsules under sunlight exposure. The intensity of the absorption peak at 490 nm in the visible region gradually decreases during sunlight exposure, while the peaks in the UV region remain unchanged (Figure 5a). These results indicate that fluorescein is readily degraded within the capsules,[14] while maintaining the molecular structure of **1** without decomposition in this experimental condition. For a comparative investigation, we have performed the photocatalytic activity experiments with the membrane solutions

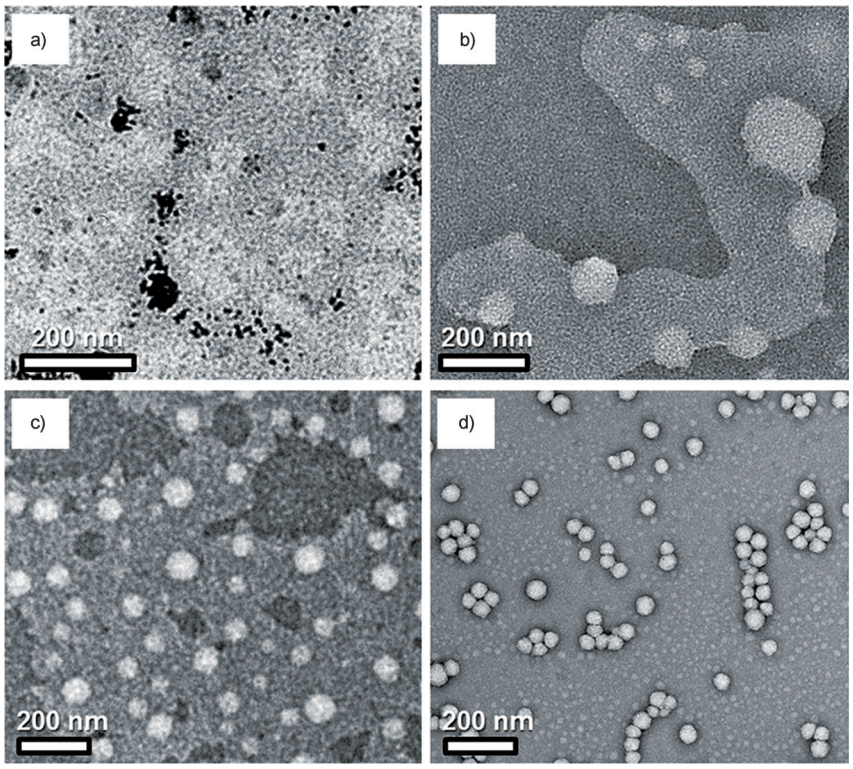

Figure 4. Negative-stain TEM images of the aqueous solutions **1** (50 μM) with 0.5 equivalents of corannulene over one month: a) 3 days; b) 7 days; c) 15 days; d) 1 month.

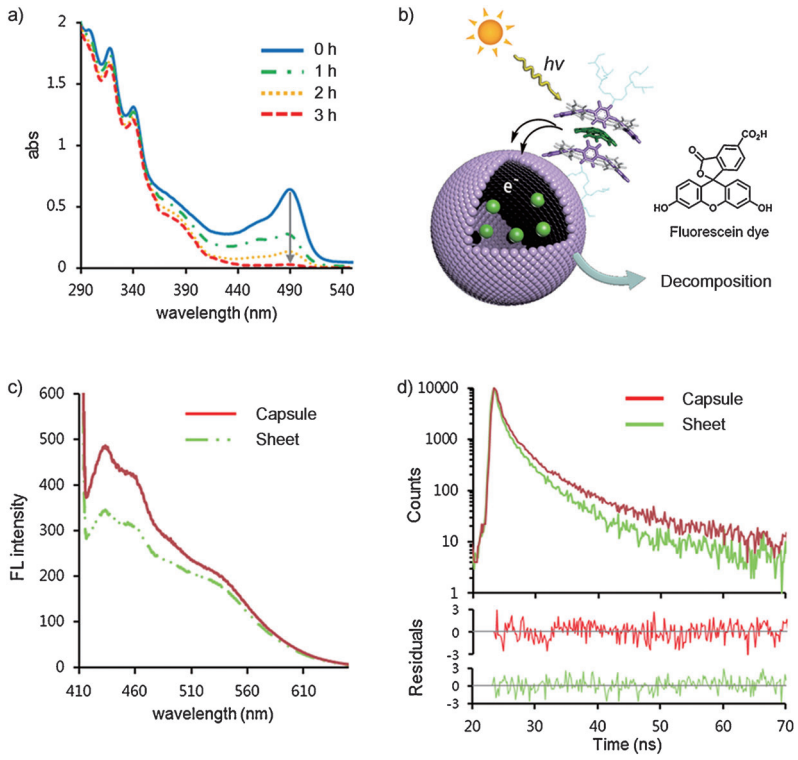

Figure 5. a) Absorption spectra after the encapsulation of fluorescein into capsule and the exposure under sunlight. b) Schematic representation of the photocatalytic decomposition of fluorescein. c) Emission spectra of aqueous solution **1** (50 μM) with corannulene (red solid line); without corannulene (green dash–dotted line) at 401 nm excitation wavelength. d) Fluorescence decays (in counts) of aqueous solution **1** (50 μM) with corannulene (red line); without corannulene (green line) at 401 nm excitation wavelength. The distribution of fit residuals is displayed on the bottom.

before corannulene intercalation (Figure S1, Supporting Information). At the same sunlight irradiation condition, the peak intensity at 490 nm remains unchanged, which suggests that the pure assembly of **1** is not active for photocatalytic degradation.

The photocatalytic activity of the suparmolecular capsules can be understood by the suppression of recombination rate from the excited state by corannulene.[15] This is reflected in the enhanced fluorescence intensity and the lifetime of the suparmolecular capsules. The fluorescence emission of the suparmolecular capsules relative to the membranes without corannulene was increased by a factor of 1.5, upon excited at 401 nm (Figure 5c), which implies the suppression of recombination rate upon the intercalation of corannulene. Time-resolved fluorescence experiments were carried out to further understand the excited-state dynamics with excitation at 401 nm (Figure 5d and Figure S2, Supporting Information). The fluorescence decay profile of the supramolecular capsule solution exhibited a multiexponential decay with longer lifetimes than those of the membrane solution, which indicates that the intercalation of corannulene leads the system to suppress recombination and thus to induce photocatalytic activity.

We have demonstrated the construction of smart supramolecular capsules from 2D aromatic membrane scission triggered by curved corannulene intercalation. The membrane structure consists of lateral arrangements of dimeric macrobicycle amphiphiles in which the intercalation of curved corannulene drives the shape of the dimeric pair to adopt a curved conformation. Consequently, this curvature of the corannulene-intercalated dimeric micelles enforces

the membrane structures to gradually break-up into discrete capsule structures through bud formation as intermediate steps. Consequently, these capsules could be considered as supramolecular capsules because the framework of the capsule consists of the lateral array of corannulene, a buckyball fragment. The resulting supramolecular capsules exhibit interesting photocatalytic activity to degrade encapsulated fluorescein dye molecules under sunlight irradiation. Such dynamic supramolecular capsules with photoresponsive characteristics hold outstanding potentials for a broad range of applications to solve future energy conversion issues.

Acknowledgements

This work was supported by 111 Project (Grant B06009), NSFC (Grant 51473062), and 1000 program.

Keywords: corannulene · membrane scission · self-assembly · supramolecular capsules · uniform hollow objects

[1] a) T. Aida, E. Meijer, S. Stupp, *Science* **2012**, *335*, 813 – 817; b) B. M. Rosen, C. J. Wilson, D. A. Wilson, M. Peterca, M. R. Imam, V. Percec, *Chem. Rev.* **2009**, *109*, 6275 – 6540; c) T. F. A. De Greef, M. M. J. Smulders, M. Wolffs, A. P. H. J. Schenning, R. P. Sijbesma, E. W. Meijer, *Chem. Rev.* **2009**, *109*, 5687 – 5754; d) X. Yan, F. Wang, B. Zheng, F. Huang, *Chem. Soc. Rev.* **2012**, *41*, 6042 – 6065; e) A. Ajayaghosh, V. K. Praveen, *Acc. Chem. Res.* **2007**, *40*, 644 – 656; f) H. Shao, J. Seifert, N. C. Romano, M. Gao, J. J. Helmus, C. P. Jaroniec, D. A. Modarelli, J. R. Parquette, *Angew. Chem. Int. Ed.* **2010**, *49*, 7688 – 7691; *Angew. Chem.* **2010**, *122*, 7854 – 7857; g) X. Zhang, S. Rehm, M. Safont-Sempere, F. Würthner, *Nat. Chem.* **2009**, *1*, 623 – 629; h) T. Ogoshi, S. Kanai, S. Fujinami, T.-a. Yamagishi, Y. Nakamoto, *J. Am. Chem. Soc.* **2008**, *130*, 5022 – 5023; i) S. Moghaddam, Y. Inoue, M. K. Gilson, *J. Am. Chem. Soc.* **2009**, *131*, 4012 – 4021; j) D. Görl, X. Zhang, F. Würthner, *Angew. Chem. Int. Ed.* **2012**, *51*, 6328 – 6348; *Angew. Chem.* **2012**, *124*, 6434 – 6455; k) X. Zhang, D. Görl, V. Stepanenko, F. Würthner, *Angew. Chem. Int. Ed.* **2014**, *53*, 1270 – 1274; *Angew. Chem.* **2014**, *126*, 1294 – 1298.

[2] a) Y. Kim, W. Li, S. Shin, M. Lee, *Acc. Chem. Res.* **2013**, *46*, 2888 – 2897; b) H.-J. Kim, T. Kim, M. Lee, *Acc. Chem. Res.* **2011**, *44*, 72 – 82; c) M. Lee, B.-K. Cho, W.-C. Zin, *Chem. Rev.* **2001**, *101*, 3869 – 3892; d) W. Li, Y. Kim, M. Lee, *Nanoscale* **2013**, *5*, 7711 – 7723; e) Z. Huang, H. Lee, E. Lee, S.-K. Kang, J.-M. Nam, M. Lee, *Nat. Commun.* **2011**, *2*, 459.

[3] a) S. Zhang, *Nat. Biotechnol.* **2003**, *21*, 1171 – 1178; b) D. Lingwood, K. Simons, *Science* **2010**, *327*, 46 – 50.

[4] a) M. Klingenberg, *Nature* **1981**, *290*, 449 – 454; b) M. Edidin, *Nat. Rev. Mol. Cell Biol.* **2003**, *4*, 414 – 418.

[5] a) B. J. Reynwar, G. Illya, V. A. Harmandaris, M. M. Müller, K. Kremer, M. Deserno, *Nature* **2007**, *447*, 461 – 464; b) J. Zimmerberg, M. M. Kozlov, *Nat. Rev. Mol. Cell Biol.* **2006**, *7*, 9 – 19; c) H. T. McMahon, J. L. Gallop, *Nature* **2005**, *438*, 590 – 596.

[6] a) V. Percec, D. A. Wilson, P. Leowanawat, C. J. Wilson, A. D. Hughes, M. S. Kaucher, D. A. Hammer, D. H. Levine, A. J. Kim, F. S. Bates, K. P. Davis, T. P. Lodge, M. L. Klein, R. H. DeVane, E. Aqad, B. M. Rosen, A. O. Argintaru, M. J. Sienkowska, K. Rissanen, S. Nummelin, J. Ropponen, *Science* **2010**, *328*, 1009 – 1014; b) V. Percec, P. Leowanawat, H.-J. Sun, O. Kulikov, C. D. Nusbaum, T. M. Tran, A. Bertin, D. A. Wilson, M. Peterca, S. Zhang, N. P. Kamat, K. Vargo, D. Moock, E. D. Johnston, D. A. Hammer, D. J. Pochan, Y. Chen, Y. M. Chabre, T. C. Shiao, M. Bergeron-Brlek, S. André, R. Roy, H.-J. Gabius, P. A. Heiney, *J. Am. Chem. Soc.* **2013**, *135*, 9055 – 9077; c) S. Zhang, H.-J. Sun, A. D. Hughes, R.-O. Moussodia, A. Bertin, Y. Chen, D. J. Pochan, P. A. Heiney, M. L. Klein, V. Percec, *Proc. Natl. Acad. Sci. USA* **2014**, *111*, 9058 – 9063; d) D. K. Smith, F. Diederich, *Chem. Eur. J.* **1998**, *4*, 1353 – 1361; e) A. Taubert, A. Napoli, W. Meier, *Curr. Opin. Chem. Biol.* **2004**, *8*, 598 – 603; f) S. Zhang, R.-O. Moussodia, H.-J. Sun, P. Leowanawat, A. Muncan, C. D. Nusbaum, K. M. Chelling, P. A. Heiney, M. L. Klein, S. André, R. Roy, H.-J. Gabius, V. Percec, *Angew. Chem. Int. Ed.* **2014**, *53*, 10899 – 10903; *Angew. Chem.* **2014**, *126*, 11079 – 11083; g) A. Barnard, D. K. Smith, *Angew. Chem. Int. Ed.* **2012**, *51*, 6572 – 6581; *Angew. Chem.* **2012**, *124*, 6676 – 6685; h) H. Jin, W. Huang, X. Zhu, Y. Zhou, D. Yan, *Chem. Soc. Rev.* **2012**, *41*, 5986 – 5997.

[7] Z. Huang, S.-K. Kang, M. Banno, T. Yamaguchi, D. Lee, C. Seok, E. Yashima, M. Lee, *Science* **2012**, *337*, 1521 – 1526.

[8] a) J.-K. Kim, E. Lee, M.-C. Kim, E. Sim, M. Lee, *J. Am. Chem. Soc.* **2009**, *131*, 17768 – 17770; b) Z. Huang, S.-K. Kang, M. Lee, *J. Mater. Chem.* **2011**, *21*, 15327 – 15331.

[9] J. K. Kim, E. Lee, Y. b. Lim, M. Lee, *Angew. Chem. Int. Ed.* **2008**, *47*, 4662 – 4666; *Angew. Chem.* **2008**, *120*, 4740 – 4744.

[10] E. Lee, J. K. Kim, M. Lee, *Angew. Chem. Int. Ed.* **2009**, *48*, 3657 – 3660; *Angew. Chem.* **2009**, *121*, 3711 – 3714.

[11] Y. Kim, S. Shin, T. Kim, D. Lee, C. Seok, M. Lee, *Angew. Chem. Int. Ed. Angew. Chem.Int. Ed.* **2013**, *52*, 6426 – 6429; *Angew. Chem.* **2013**, *125*, 6554 – 6557.

[12] a) H. T. McMahon, E. Boucrot, *Nat. Rev. Mol. Cell Biol.* **2011**, *12*, 517 – 533; b) J. Weinberg, D. G. Drubin, *Trends Cell Biol.* **2012**, *22*, 1 – 13; c) J. S. Bonifacino, B. S. Glick, *Cell* **2004**, *116*, 153 – 166; d) M. Kaksonen, C. P. Toret, D. G. Drubin, *Cell* **2005**, *123*, 305 – 320; e) E. J. Ungewickell, L. Hinrichsen, *Curr. Opin. Cell Biol.* **2007**, *19*, 417 – 425.

[13] a) A. Ayalon, M. Rabinovitz, P.-C. Cheng, L. T. Scott, *Angew. Chem. Int. Ed. Engl.* **1992**, *31*, 1636 – 1637; *Angew. Chem.* **1992**, *104*, 1691 – 1692; b) L. Zoppi, L. Martin-Samos, K. K. Baldridge, *J. Am. Chem. Soc.* **2011**, *133*, 14002 – 14009; c) Y.-T. Wu, D. Bandera, R. Maag, A. Linden, K. K. Baldridge, J. S. Siegel, *J. Am. Chem. Soc.* **2008**, *130*, 10729 – 10739; d) Q. Li, B. Guo, J. Yu, J. Ran, B. Zhang, H. Yan, J. R. Gong, *J. Am. Chem. Soc.* **2011**, *133*, 10878 – 10884; e) C. Bruno, R. Benassi, A. Passalacqua, F. Paolucci, C. Fontanesi, M. Marcaccio, E. A. Jackson, L. T. Scott, *J. Phys. Chem. B* **2009**, *113*, 1954 – 1962; f) G. Valenti, C. Bruno, S. Rapino, A. Fiorani, E. A. Jackson, L. T. Scott, F. Paolucci, M. Marcaccio, *J. Phys. Chem. C* **2010**, *114*, 19467 – 19472.

[14] LCMS measurements showed that the peak associated with fluorescein dye disappears completely after 3 h sunlight exposure (Figure S5, Supporting Information).

[15] M. Yamaji, K. Takehira, T. Mikoshiba, S. Tojo, Y. Okada, M. Fujitsuka, T. Majima, S. Tobita, J. Nishimura, *Chem. Phys. Lett.* **2006**, *425*, 53 – 57.

Received: January 10, 2015
Published online on ■■ ■■, 0000

COMMUNICATION

Self-Assembly

*Y. Kim, M. Lee**

■■ – ■■

Supramolecular Capsules from Bilayer Membrane Scission Driven by Corannulene

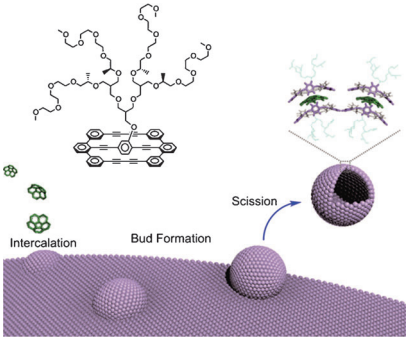

Self-assembly of polyaromatic systems has proved to be a powerful technique to construct nanoscale optoelectronic materials. However, attempts to develop self-assembled nanomaterials guided by pristine polyaromatic molecules have been limited. Here the construction of photoactive nanocapsules through the scission of an aromatic bilayer membrane driven by curved corannulene intercalation is reported (see figure).